
**E-ISSN:** 2664-6773
**P-ISSN:** 2664-6765
**Impact Factor:** RJIF 5.6
IJCBS 2025; 7(1): 01-10
www.chemicaljournal.org
Received: 04-10-2024
Accepted: 10-11-2024

**Aymen Hasan Abdulrazzaq**
Senior Chief Chemist, Department of Applied Sciences, Biochemical Technology University of Technology, Baghdad, Iraq

**Corresponding Author:**
**Aymen Hasan Abdulrazzaq**
Senior Chief Chemist, Department of Applied Sciences, Biochemical Technology University of Technology, Baghdad, Iraq

# Using nanominutes to enhance residual oil production through polymer flooding

**Aymen Hasan Abdulrazzaq**

**DOI:** https://doi.org/10.33545/26646765.2025.v7.i1a.114

**Abstract**
Polymer solutions containing nanoparticles could potentially provide a promising direction for improving the efficiency of oil recovery; however, their exact action and efficiency are still not well-studied. To achieve this objective, a detailed examination of the rheological properties and capillary dynamics (i.e., interfacial tension and contact angle) exhibited by the nanoparticles during oil recovery in polymer processes is conducted in this study. The technique employed includes sequential injection of water, polymer and nanoparticles using synthesized nanosilica (SiO2) as well as nano-aluminium oxide (Al2O3) to evaluate regeneration of crude oil from reservoir rocks under different experimental conditions. The results indicate that water loss is influenced by mobility ratio of polymer-nanoparticles leading into reduction in retention capacity and capillarity strength but increase in viscoelasticity of the polymer itself. Particularly, polymer-SiO2 flooding showed higher percentage of oil recovery than other scenarios whose capillary strength was compromised due to structural breakdown pressure. In addition, when determining relative permeabilities residual saturation (Sor) was found to be 29% while water relative permability (Krw) equalled 0.3%. However, for polymer-nanoparticle mixture, these values were changed into 12% and 0.005%, respectively. The contact angle after the treatment of the polymer was lower, with 21 and 29 degrees, respectively. The addition of the nanoparticles decreased it even more; this should correspond to an increase in hydrophilicity. Beyond the concentration of 2000 mg L−1 of SiO2, no more significant changes were observed. These findings indicate that such a nanoparticle-enhanced polymer solution may serve as a feasible alternative to the more conventional chemical enhanced oil recovery techniques, especially in applications where a shift in oil mobility and increased recovery efficiencies under reservoir conditions are required.

**Keywords:** Nanominutes, enhance residual oil production, polymer flooding, oil

## 1. Introduction
The oil industry is actively seeking to enhance production from underground hydrocarbon fields in response to the increasing global energy demand across various sectors, including the need for crude oil and its derivatives. To meet this sustainable demand, the implementation of modern technologies and innovative developments is essential. However, petroleum industries face significant challenges, as natural mechanical drives often prove inefficient. Advancements in oil recovery techniques are crucial for increasing oil accumulation. Various enhanced oil recovery (EOR) methods, frequently discussed in the literature, focus on chemical approaches to boost oil production rates in porous media. Among these, polymer flooding has emerged as an effective migration technique, enhancing water solubility, and facilitating the rapid movement of oil through porous structures. High-performance polymers, such as polyacrylamide (PAM) and partially hydrolyzed polyacrylamide (HPAM), play a vital role in improving oil recovery by increasing humidity, enhancing water conversion, and reducing interfacial pressure.
For optimal performance in polymer flooding systems, several factors regarding polymer properties must be considered. First, the carbon chains in the polymer solution should be devoid of –O– groups to ensure high thermal stability. Second, incorporating a negatively charged ionic hydrophilic group can minimize rock surface adsorption. Third, the polymer must exhibit viscous properties to ensure effective performance during flooding processes. Lastly, the presence of a nonionic hydrophilic group is crucial for maintaining the stability of the formulation. Among these considerations, HPAM has demonstrated superior efficacy in enhancing oil recovery compared to other polymers.
The integration of nanoparticles with organic polymers presents an intriguing opportunity to leverage their inorganic characteristics, potentially synergizing the benefits of both materials to improve oil recovery performance. The formation of hydrogen bonds between polymers and

nanoparticles can enhance the rheological properties of polymer-nanoparticle aqueous solutions, particularly under high salt concentrations and elevated temperatures. Incorporating nanoparticles into these systems is expected to significantly influence water exchange and reduce interfacial tension, while also enhancing the viscous properties of the polymer. This combination facilitates the active flow of oil through porous media.

Thus, the amalgamation of polymers and nanoparticles offers a promising alternative to conventional chemical methods, such as polymer-surfactant and alkaline-polymer-surfactant systems. Additionally, the economic advantages of producing nanoparticles are noteworthy, as their production costs are significantly lower than those associated with chemical syntheses, including surfactants and foams. Previous studies, such as those conducted by Zoo *et al*. (2006) and Ogolo *et al*. (2012), have experimentally demonstrated the substantial impact of nanoparticle addition on oil recovery, concluding that nanoparticles can effectively reduce interfacial tension, promote emulsion stability, enhance water exchange, and improve overall formulation stability.

## 2. Materials and Methods

### 2.1. Materials

In this study, crude oils with viscosities of 0.02 and 23 centipoise (cP), along with API gravities, were utilized. To ensure consistency with the submitted applications, synthetic salts were prepared using a solution containing 6000 milligrams per liter (mg L−1) of potassium chloride (KCl). The choice of KCl was based on its ability to produce homogeneous salts, while also minimizing the presence of monovalent ions, which can potentially impact polymer stability. sThe partially hydrolyzed polyacrylamide (HPAM) polymer employed in this study was synthesized with both carboxyl and amide functional groups, and had a molecular weight of 7 million Daltons (MDa). The degree of hydrolysis in HPAM was approximately 30%, which is a common value for polymers used in enhanced oil recovery applications. Aluminum oxide (Al2O3) and silicon dioxide (SiO2) nanoparticles with an average thickness of 7 nanometers (nm) were selected for this investigation. These nanoparticle types have been extensively studied in previous literature and have shown promising results in improving oil recovery efficiency [62-64].

Sandbags were fabricated with an average porosity of 25% and a permeability range of 450 to 680 millidarcies (mD). The sand composition consisted of 2% chlorite, 3% kaolinite, 1% illite, and 6% clay. Various grain sizes, ranging from 20 to 140, were sorted to create artificial sandbags with consistent petrophysical characteristics. These sandbags were specifically tailored to match the permeability and porosity of the reservoir. Subsequently, the sand was immersed in a 5% hydrochloric acid (HCl) solution for a duration of one day to eliminate contaminants. In the final stage, the sand was dried and compacted under a pressure of 25 megapascals (MPa) before being integrated into the flooding system.

### 2.2. Methods

Figure 1 illustrates the testing apparatus designed for spontaneous flooding. This setup utilizes a polymer/nanoparticle mixture, which is prepared as a liquid solvent before being injected into the system. The injection apparatus was placed in a drying oven (DZLG-9123A Drying Oven, EJER TECH, Pingyao, China) to maintain the reservoir temperature at 333 K, while the system's pressure was regulated to approximately 12 bed volumes. An 8 PV oil and synthetic salt solution was injected at a rate of 0.003 m³/min to initiate the flooding process. The sand pack was filled to its maximum capacity. To evaluate oil recovery across different scenarios, the system executed a series of injection protocols at a reduced rate of 0.001 m³/min, as the sandbags required drying and cleaning after each test.

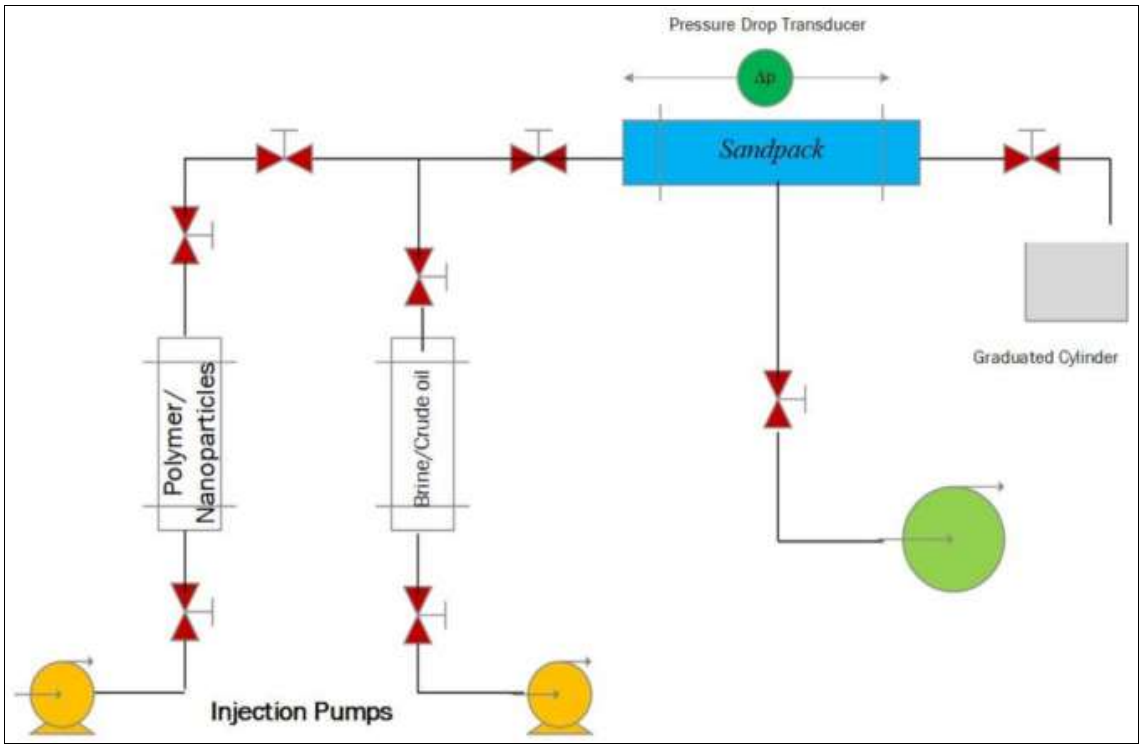


**Fig 1:** Schematic Diagram of the Polymer/Nanoparticle Flooding Testing Apparatus

To assess the interfacial tension of various nanoparticle concentrations, an aqueous polymer solution was prepared as the test phase. The results were compared to the interfacial tension between the water-SiO2 system and the oil phase to establish a baseline. Thermodynamic equilibrium conditions were maintained at a constant ambient temperature of 298 K in the laboratory setting for a duration of one day. The use of a drying oven (DZLG-9123A, EJER TECH, Pingyao, China)

ensured that inaccuracies were minimized, thereby optimizing process efficiency, and reducing experimental error.

The residual resistance factor (RRF) quantifies the resistance to excess flow (Polymer) during the injection of polymer solutions through porous media, which can diminish the effective cross-sectional area available for flow. This parameter can be calculated by comparing the permeability values measured before and after polymer flooding. The RRF provides a measure of the polymer's ability to reduce the permeability of the porous medium, which is a crucial consideration in the design and optimization of polymer flooding processes.

Relative permeability curves serve as a method to illustrate the impact of capillary properties on the flow of water and oil through porous media. To evaluate the permeability of each phase, synthetic salts were introduced into the system to establish the residual oil saturation. Subsequently, an aqueous solution was injected, and finally, water was added to displace the remaining oil and achieve maximum recovery.

The contact angle was assessed at 333 K to evaluate the influence of nanoparticles on capillary potential and moisture variations. Following the washing and cleaning of the samples, they were submerged in nanoparticle solutions for a duration of one day and underwent aging regeneration in an oil-wet environment to facilitate contact angle measurements. This process involved continuous stirring at 500 rpm, after which the fluid contact angle was determined using Layout 2015 software.

To assess the apparent wettability, the polymer solution was injected at varying flow rates. Once a stable flow was achieved within the system, the apparent viscosity of the polymer was determined using the Darcy equation:

$$\upsilon = \frac{Q}{S\phi} \quad (1)$$

where υ is the apparent viscosity, S is the core cross section, Q is the flow rate, and ϕ is the porosity. The shear rate can be calculated using the following equation:

$$\gamma_{pm} = 4\alpha\frac{\upsilon}{r} \quad (2)$$

where α varies based on different reservoir conditions and is assumed to be equal to 1.

## 3. Results and Discussion

The interfacial tension between oil-water and oil-polymer systems was evaluated in the presence of a significant concentration of SiO2 nanoparticles under controlled laboratory conditions, as illustrated in Figure 2. Notably, the presence of SiO2 nanoparticles led to a reduction in interfacial tension for both oil-water and oil-polymer systems as the concentration of nanoparticles increased. Sun *et al.* (2017) reported a similar decrease in the oil-water phase interfacial tension, attributing it to a reduction in Gibbs energy resulting from the positioning of nanoparticles at the oil-water interface. Conversely, the interfacial tension for the oil-polymer system was marginally lower, as the aggregation of nanoparticles at the oil-polymer interface was less pronounced, leading to diminished interfacial fluctuations with an increase in nanoparticle concentration.

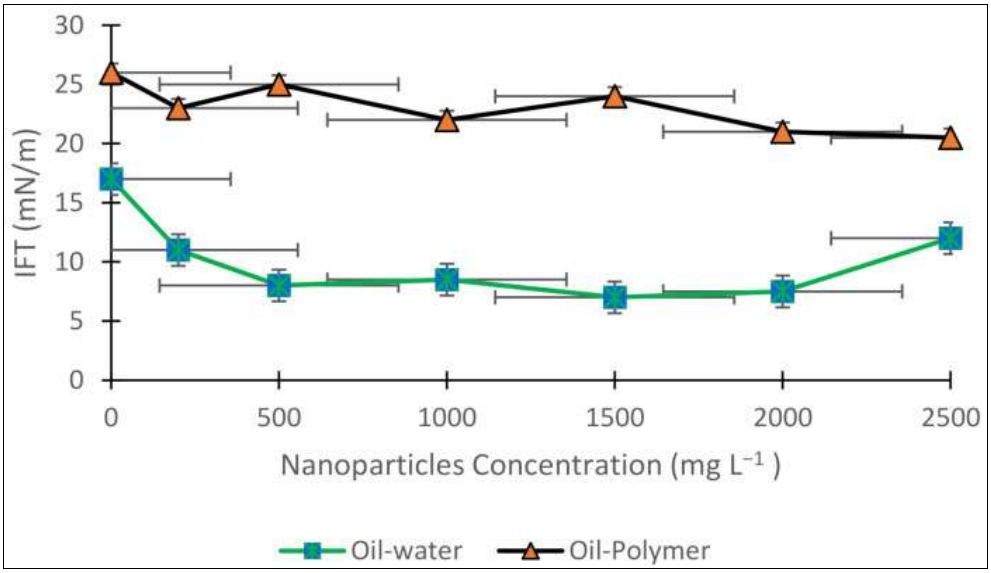


**Fig 2:** Interfacial Tension for Oil-Water and Oil-Polymer Systems with $SiO_2$ Nanoparticles

### 3.2. Contact Angle

Surface roughness affects the development of the interface hysteresis, which is described by means of the contact angle. That is why contact angle measurements are usually conducted on smooth surfaces to obtain reliable and true values. Landslides in wettability, relative pressure curves and porosity rely heavily on the contact angle. In the meantime, these aspects significantly influence the ability of crude oil recovery considering their impacts on water-water or oil-water properties at the rock-wellbore interface [76, 77]. Nanoparticles including SiO2 were used to investigate the effect of several types of nanoparticles on polymer and water surfaces' contact angles. It was realized that before treatment, hydrolysis happens on rock surfaces while after treatment it changed from one form to another as shown below in figure 3 due to adsorption of nanoparticles leading to lower contact angles. Consequently, minimum contact angles for water and polymer treatments were about 21° and 29°, respectively. The attached nanoparticles to surface increased hydrophilicity thus lowering further contact angle hence improved polymer wettability. Beyond that, there was no notable change in the value of SiO2 concentration above 2000 mg. $L^{-1}$ increasing the possibility of contact angle remaining constant. These findings were consistent with theoretical calculations reported in previous publications [78-80].

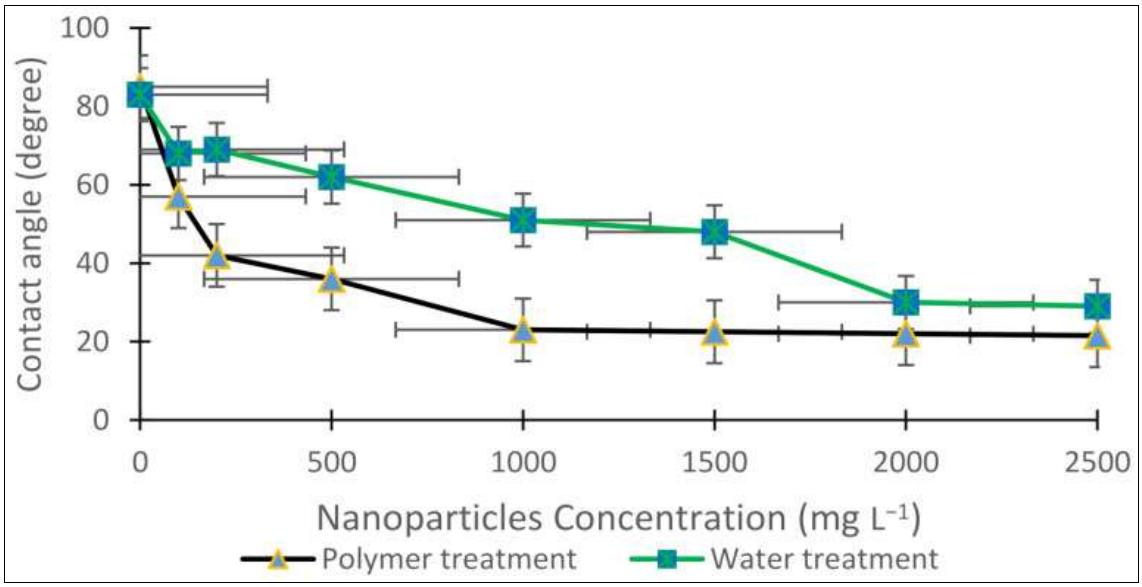


**Fig 3:** Effect of Nanoparticles on Contact Angle for Polymer and Water Treatments

### 3.3. Viscosity

Interestingly, it is observed that the apparent viscosity of polymer solutions is being affected by an increasing trend due to the incorporation of nanoparticles (SiO2 and Al2O3). As depicted in Figure 4, nanoparticles contributed to a rise in the viscosity and shear thinning of the polymer solution. This can be considered as a reasonable prediction for the shear rate at 10 s−1 because of the lower power model. In these earlier papers, 81-83 have connected such operating procedure with flowing behavior of microstructures made from polymers.

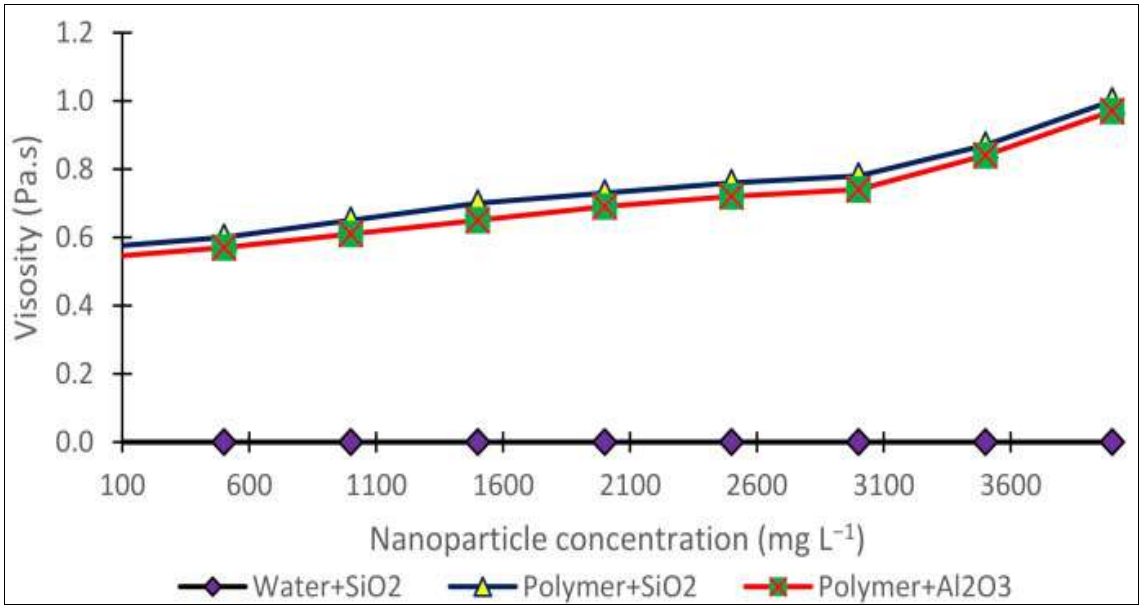


**Fig 4:** Variation in Apparent Viscosity of Polymer Solutions with Nanoparticle Addition

### 3.4. Relative Permeability Curves

Figure 5 shows the permeability curves due to water and polymer flooding when nanoparticles are present. The rise in the quantity of residual oil saturation (Sor) corresponds with a decline in water permeability; Sor and Krw values for the polymer solution are 29% and 0.3%, respectively. For the polymer-nanoparticle solution, Sor and Krw are recorded at 12% and 0.005%, respectively. Thus, there is an apparent decrease for both parameters with and without nanoparticles. Therefore, although there is a lowering of pore strength along with increased oil recovery through water-water-rock interactions owing to presence of nanoparticles, ultimate Sor and Krw transformation involves such viscosity changes that transform from medium strength to high strength water not complying to condemnations. This issue has been considered earlier as well [68, 84, 85].

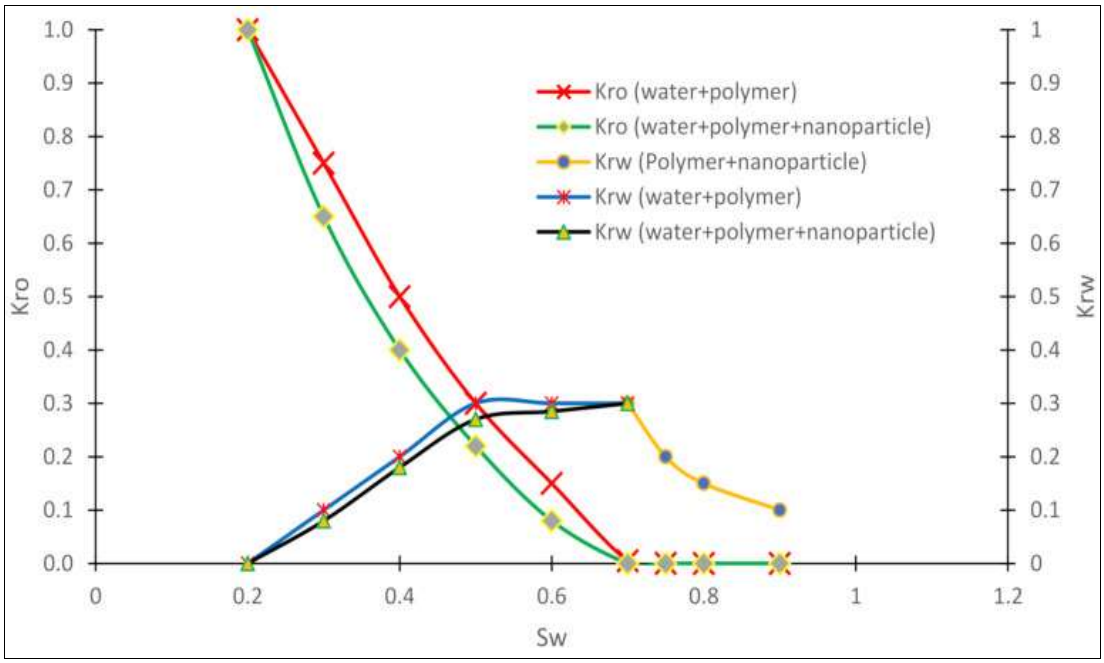


**Fig 5:** Relative Permeability Curves for Polymer and Nanoparticle Flooding

### 3.5. Residual Resistance Factor

The residual resistivity factor serves as a comparative measure of rock surface exposure before and after polymer flooding. This factor indicates a reduction in rock-water interactions and cross-sectional flow. Following a shear rate of 100 $s^{-1}$, the residual resistance factor stabilized, reaching a plateau. An increase in the shear rate, threefold, revealed irregularities in the polymer nanoparticle behavior. In this study, a polymer solution of hydrolyzed polyacrylamide (HPAM) at a concentration of 500 mg/L was utilized. For the Al2O3-polymer solution (500 mg/L HPAM and 3000 mg/L Al2O3), the partial resistance was approximately 6, while for the SiO2-polymer solution (500 mg/L HPAM and 3000 mg/L SiO2), it was around 5.5, with some instances showing a value of 3.8. The weaker interactions and electrostatic repulsion observed in ionic sandstone rocks contribute to decreased polymer retention as it flows through the porous medium, as illustrated in Figure 6 [86, 87].

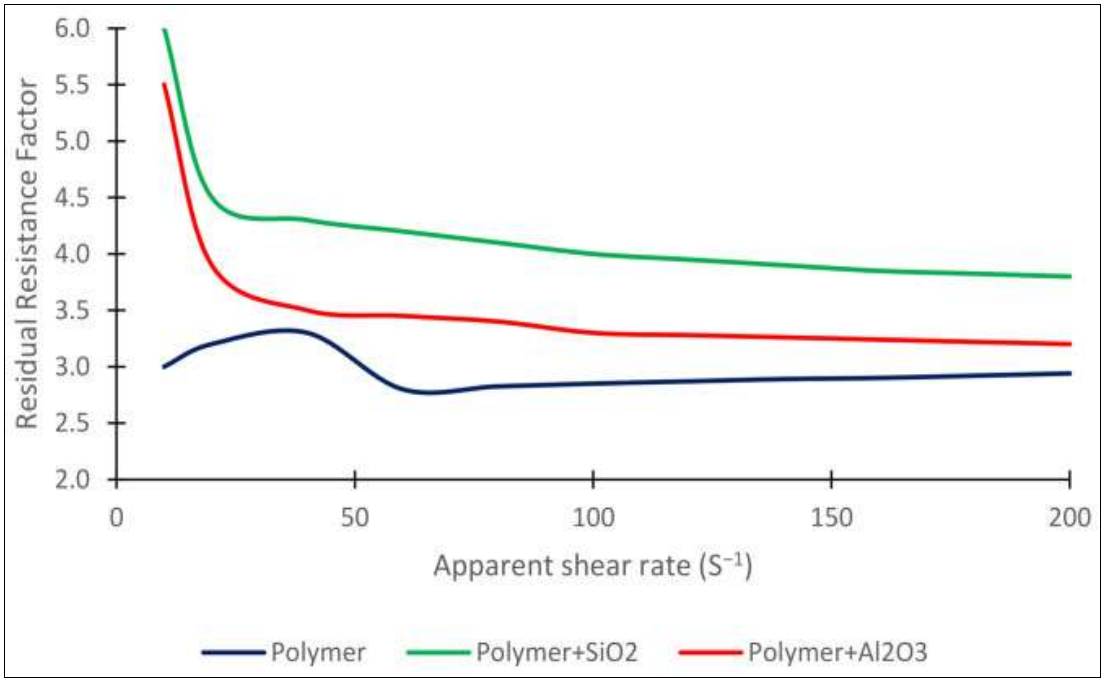


**Fig 6:** Residual Resistance Factor for Various Polymer-Nanoparticle Solutions

**3.6. Pressure Drop:** Figure 7 illustrates the pressure drop profiles during water and polymer flooding in the absence of nanoparticles. It is evident that the pressure drop remained low throughout the flooding process. During the initial stages of polymer flooding, the pressure drop exhibited minor fluctuations but gradually increased with the injection of pore volumes until it reached a maximum of approximately 0.055 MPa. This pressure drop can be attributed to the increased viscosity of the polymer solution compared to water, which leads to a higher resistance to flow through the porous medium. However, the overall pressure drop remained within a manageable range, indicating that the polymer flooding process was not significantly hindered by excessive pressure buildup in the absence of nanoparticles.

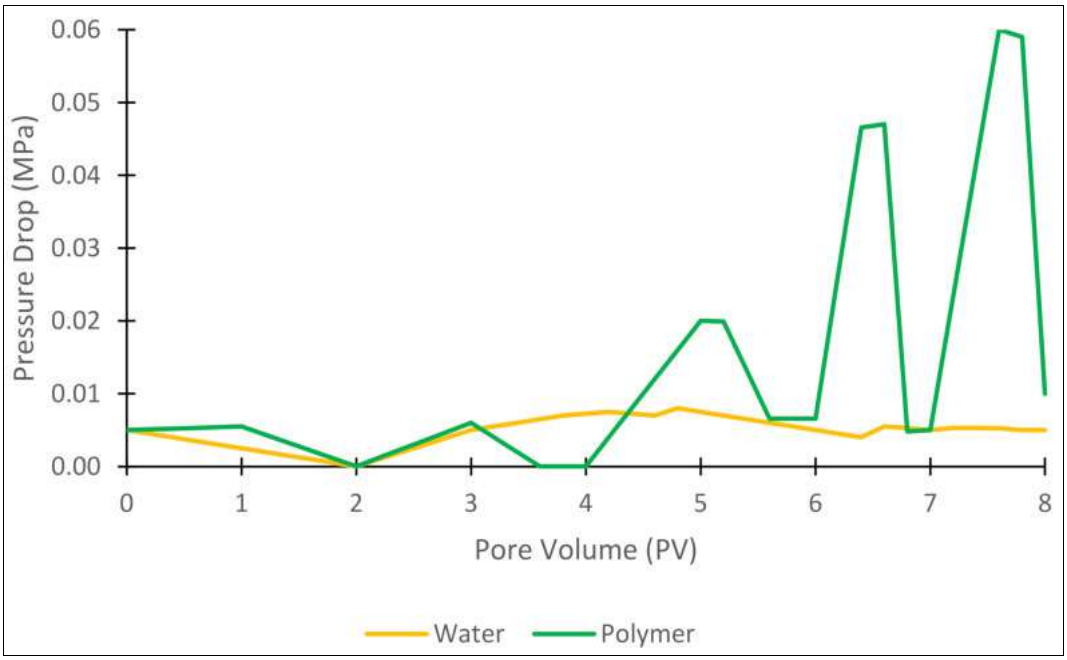


**Fig 7:** Pressure Drop Profiles during Polymer Flooding without Nanoparticles

### 3.7. Oil Recovery Factor

Original oil in place (OOIP) refers to the total volume of oil contained within a hydrocarbon reservoir, which can be calculated using the following equation:

$$OOIP = 7758Vb\,(NTG)\varphi\, S_o/B_o \quad (3)$$

in this equation, ϕ represents the porosity, So*So* denotes the oil saturation, Bois the oil formation volume factor, NTG indicates the ratio of net to gross volume, and Vbis the bulk volume, which can be geometrically derived from the dimensions of the reservoir. The recovery factor of oil introduced relative to OOIP demonstrates a direct correlation between porosity and oil recovery potential [33, 34]. Higher porosity levels facilitate improved oil recovery, as the oil phase can flow more freely through the porous medium. To assess oil recovery, nanoparticles were sequentially injected into water and polymer solutions, resulting in oil recovery rates of 48%, 58%, 63%, and 67% for each respective flooding scenario: water flood, polymer flood, and polymer-SiO2 flood, as illustrated in Figure 8. This data indicates that the polymer-SiO2 flooding method yields superior oil recovery compared to the other approaches, primarily due to a reduction in viscosity caused by the breakdown of the system under stress.

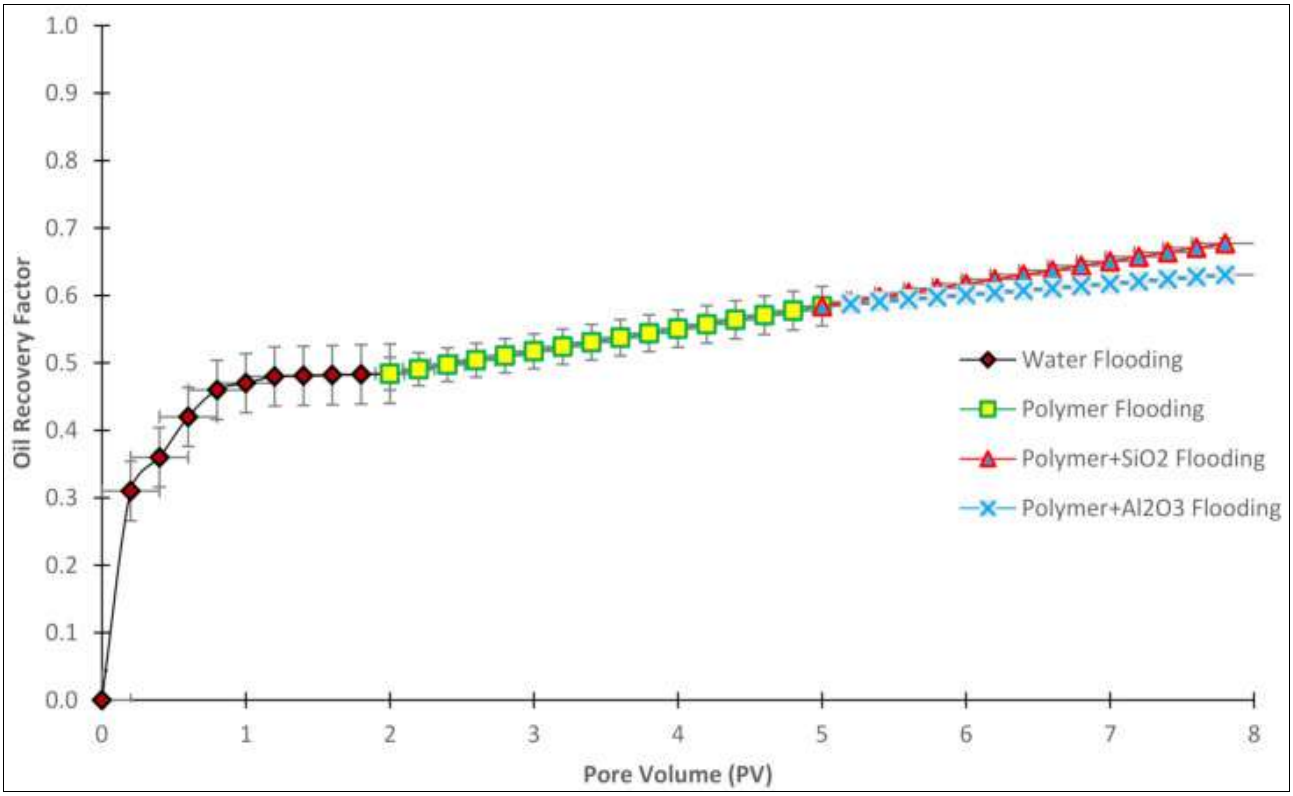


**Fig 8:** Oil Recovery Factor for Different Flooding Scenarios

## 4. Conclusions

The significant demand for crude oil and its derivatives across various industries underscores the necessity of enhancing cumulative oil production from hydrocarbon reservoirs. The oil recovery rates for different flooding methods are as follows: water floods at 48%, polymer floods at 58%, polymer-Al2O3 floods at 63%, and polymer-SiO2 floods at 67%. Consequently, polymer-SiO2 flooding demonstrates superior oil recovery compared to the other methods, even though it may reduce capillary strength due to structural breakdown pressure. Notably, the pressure drop resulting from pore volume injection remained stable, with a significant drop of approximately 0.005 MPa observed. During the initial phases of polymer flooding, the pressure drop exhibited slight variability, increasing with the volume of injected pore fluid, reaching a maximum of 0.055 MPa. The incorporation of nanoparticles into the polymer solution improved viscosity and exhibited shear-thinning behavior, which is linked to the flow dynamics of the polymer microstructures. With respect to the presence of SiO2 nanoparticles, increasing the concentrations of oil-water and oil-polymer nanoparticles led to a slight reduction in interfacial tension. This decrease was more pronounced in the oil-polymer system, where the placement of nanoparticles at the oil-polymer interface became limited, resulting in reduced changes in the surface area of the interface. Importantly, these changes were not associated with an increase in surface tension, and the contact distance for polymer treatments in the presence of membranes was diminished. As a result, the contact angle did not vary significantly beyond a SiO2 concentration of 2000 mg $L^{-1}$.

## 5. References


1. Wang MR, Deng L, Liu GC, Wen L, Wang JG, Huang KB, *et al*. Porous organic polymer-derived nanopalladium catalysts for chemoselective synthesis of antitumor benzofuro[2,3-b]pyrazine from 2-Bromophenol and Isonitriles. Org Lett. 2019;21(14):5404-5408. DOI:10.1021/acs.orglett.9b01230.
2. Zuo C, Chen Q, Tian L, Waller L, Asundi A. Transport of intensity phase retrieval and computational imaging for partially coherent fields: The phase space perspective. Opt Lasers Eng. 2015;69:53-63. DOI:10.1016/j.optlaseng.2015.03.006.
3. Zhang H, Guan W, Zhang L, Guan X, Wang S. Degradation of an Organic Dye by Bisulfite Catalytically Activated with Iron Manganese Oxides: The Role of Superoxide Radicals. ACS Omega. 2020;5(25):15159-15168. DOI:10.1021/acsomega.0c01257.
4. Zhang H, Sun M, Song L, Guo J, Zhang L. Fate of NaClO and membrane foulants during in-situ cleaning of membrane bioreactors: Combined effect on thermodynamic properties of sludge. Biochem Eng J. 2019;146:1-9. DOI:10.1016/j.bej.2019.04.016.
5. Sun M, Yan L, Zhang L, Song L, Guo J, Zhang H. New insights into the rapid formation of initial membrane fouling after in-situ cleaning in a membrane bioreactor. Process Biochem. 2019;84:57-65. DOI:10.1016/j.procbio.2019.01.004.
6. Zhang K, Huo Q, Zhou YY, Wang HH, Li GP, Wang YW, *et al*. Textiles/metal-organic frameworks composites as flexible air filters for efficient particulate matter removal. ACS Appl Mater Interfaces. 2019;11(24):21987-21996. DOI:10.1021/acsami.9b01734.
7. Duan Z, Li C, Zhang Y, Dong L, Bai X, Yang M, *et al*. Milling surface roughness for 7050 aluminum alloy cavities influenced by nozzle position of nanofluid minimum quantity lubrication. Chin J Aeronaut. 2020;33(2):592-599. DOI:10.1016/j.cja.2020.04.029.
8. Zhang J, Wu W, Li C, Yang M, Zhang Y, Jia D, *et al*. Convective heat transfer coefficient model under nanofluid minimum quantity lubrication coupled with cryogenic air grinding Ti–6Al–4V. Int J Precis Eng Manuf Green Technol. 2020;7(4):767-779. DOI:10.1007/s40684-020-00268-6.
9. Gao T, Li C, Jia D, Zhang Y, Yang M, Wang X, *et al*. Surface morphology assessment of CFRP transverse grinding using CNT nanofluid minimum quantity lubrication. J Clean Prod. 2020;276:123328. DOI:10.1016/j.jclepro.2020.123328.
10. Sui M, Li C, Wu W, Yang M, Ali HM, Zhang Y, *et al*. Temperature of grinding carbide with castor oil-based MoS2 nanofluid minimum quantity lubrication. J Therm Sci Eng Appl. 2021;13(2):021008. DOI:10.1115/1.4049982.
11. Mao QF, Shang-Guan ZF, Chen HL, Huang K. Immunoregulatory role of IL-2/STAT5/CD4+ CD25+ Foxp3 Treg pathway in the pathogenesis of chronic osteomyelitis. Ann Transl Med. 2019;7(12):307. DOI:10.21037/atm.2019.07.45.
12. Huang K, Ge S. The anti-CXCL4 antibody depletes CD4 (+) CD25 (+) FOXP3 (+) regulatory T cells in CD4+ T cells from chronic osteomyelitis patients by the STAT5 pathway. Ann Palliat Med. 2020;9(6):2723-2730. DOI:10.21037/apm-20-166.
13. Zheng Y, Yu Y, Lin W, Jin Y, Yong Q, Huang C. Enhancing the enzymatic digestibility of bamboo residues by biphasic phenoxyethanol-acid pretreatment. Bioresour Technol. 2021;325:124691. DOI:10.1016/j.biortech.2021.124691.
14. Peng X, He H, Liu Q, She K, Zhang B, Wang H, *et al*. Photocatalyst-controlled and visible light-enabled selective oxidation of pyridinium salts. Sci China Chem. 2021;64(7):1006-1013. DOI:10.1007/s11426-020-9958-6.
15. Huang C, Zheng Y, Lin W, Shi Y, Huang G, Yong Q. Removal of fermentation inhibitors from pre-hydrolysis liquor using polystyrene divinylbenzene resin. Biotechnol Biofuels. 2020;13:143. DOI:10.1186/s13068-020-01828-3.
16. Lin W, Xing S, Jin Y, Lu X, Huang C, Yong Q. Insight into understanding the performance of deep eutectic solvent pretreatment on improving enzymatic digestibility of bamboo residues. Bioresour Technol. 2020;306:123163. DOI:10.1016/j.biortech.2020.123163.
17. Zhang Y, Li C, Jia D, Zhang D, Zhang X. Experimental evaluation of the lubrication performance of MoS2/CNT nanofluid for minimal quantity lubrication in Ni-based alloy grinding. Int J Mach Tools Manuf. 2015;93:76-85. DOI:10.1016/j.ijmachtools.2015.09.003.
18. Zuo C, Sun J, Li J, Zhang J, Asundi A, Chen Q. High-resolution transport-of-intensity quantitative phase microscopy with annular illumination. Sci Rep. 2017;7:46611. DOI:10.1038/s41598-017-06837-1.
19. Huang WY, Wang GQ, Li WH, Li TT, Ji GJ, Ren SC, *et al*. Porous ligand creates new reaction route: Bifunctional single-atom palladium catalyst for selective distannylation of terminal alkynes. Chem. 2020;6(1):147-156. DOI:10.1016/j.chempr.2020.06.020.
20. Qiao YX, Sheng SL, Zhang LM, Chen J, Yang LL, Zhou HL, *et al*. Friction and wear behaviors of a high nitrogen austenitic stainless steel Fe-19Cr-15Mn-0.66N. J Min Metall Sect B Metall. 2021;57(1):9-17. DOI:10.2298/JMMB201026025Q.
21. Wang P, Li Z, Xie Q, Duan W, Zhang X, Han H. A passive anti-icing strategy based on a superhydrophobic mesh with extremely low ice adhesion strength. J Bionic Eng. 2021;18(1):22-31. DOI:10.1007/s42235-021-0012-

4.
22. Kazemi A, Yang S. Effects of magnesium dopants on grain boundary migration in aluminum-magnesium alloys. Comput Mater Sci. 2021;187:110130. DOI:10.1016/j.commatsci.2020.110130.
23. Kazemi A, Yang S. Atomistic study of the effect of magnesium dopants on the strength of nanocrystalline aluminum. JOM. 2019;71(12):4311-4318. DOI:10.1007/s11837-019-03373-3.
24. Zheng L, Yu P, Zhang Y, Wang P, Yan W, Guo B, *et al*. Evaluating the bio-application of biomacromolecule of lignin-carbohydrate complexes (LCC) from wheat straw in bone metabolism via ROS scavenging. Int J Biol Macromol. 2021;169:185-194. DOI:10.1016/j.ijbiomac.2021.01.103.
25. Davarpanah A, Mirshekari B, Jafari Behbahani T, Hemmati M. Integrated production logging tools approach for convenient experimental individual layer permeability measurements in a multi-layered fractured reservoir. J Pet Explor Prod Technol. 2018;8(4):1115-1127. DOI:10.1007/s13202-017-0422-3.
26. Hu X, Li M, Peng C, Davarpanah A. Hybrid thermal-chemical enhanced oil recovery methods: An experimental study for tight reservoirs. Symmetry. 2020;12(6):947. DOI:10.3390/sym12060947.
27. Davarpanah A. Parametric study of polymer-nanoparticles-assisted injectivity performance for axisymmetric two-phase flow in EOR processes. Nanomaterials. 2020;10(9):1818. DOI:10.3390/nano10091818.
28. Hu X, Xie J, Cai W, Wang R, Davarpanah A. Thermodynamic effects of cycling carbon dioxide injectivity in shale reservoirs. J Pet Sci Eng. 2020;193:107717. DOI:10.1016/j.petrol.2020.107717.
29. Davarpanah A. A feasible visual investigation for associative foam > polymer injectivity performances in the oil recovery enhancement. Eur Polym J. 2018;107:232-240. DOI:10.1016/j.eurpolymj.2018.06.017.
30. Yang Y, Yao J, Wang C, Gao Y, Zhang Q, An S, *et al*. New pore space characterization method of shale matrix formation by considering organic and inorganic pores. J Nat Gas Sci Eng. 2015;26:706-718. DOI:10.1016/j.jngse.2015.08.017
31. Zhang K, Zhang J, Ma X, Yao C, Zhang L, Yang Y, *et al*. History matching of naturally fractured reservoirs using a deep sparse autoencoder. SPE J; c2021. DOI: 10.2118/205340-PA.
32. Nesic S, Zolotukhin A, Mitrovic V, Govedarica D, Davarpanah A. An analytical model to predict the effects of suspended solids in injected water on the oil displacement efficiency during waterflooding. Processes. 2020;8:659. DOI: 10.3390/pr8060659.
33. Davarpanah A, Mirshekari B. Experimental investigation and mathematical modeling of gas diffusivity by carbon dioxide and methane kinetic adsorption. Ind Eng Chem Res. 2019. DOI: 10.1021/acs.iecr.9b01920.
34. Mazarei M, Davarpanah A, Ebadati A, Mirshekari B. The feasibility analysis of underground gas storage during an integration of improved condensate recovery processes. J Pet Explor Prod Technol. 2019. DOI: 10.1007/s13202-018-0470-3.
35. Pan F, Zhang Z, Zhang X, Davarpanah A. Impact of anionic and cationic surfactants interfacial tension on the oil recovery enhancement. Powder Technol; c2020. DOI: 10.1016/j.powtec.2020.06.033.
36. Jia K, Feng Q, Davarpanah A. Effect of anionic and non-anionic surfactants on the adsorption density. Pet Sci Technol; c2021. DOI: 10.1080/10916466.2021.1893331.
37. Esfandyari H, Moghani A, Esmaeilzadeh F, Davarpanah A. A laboratory approach to measure carbonate rocks' adsorption density by surfactant and polymer. Math Probl Eng. 2021. DOI: 10.1155/2021/5539245.
38. Sepahvand T, Etemad V, Matinizade M, Shirvany A. Symbiosis of AMF with growth modulation and antioxidant capacity of Caucasian Hackberry (*Celtis Caucasica* L.) seedlings under drought stress. Cent Asian J Environ Sci Technol Innov. 2021, 2. DOI: 10.22034/CAJESTI.2021.01.03.
39. Jalali Sarvestani M, Charehjou P. Fullerene (C20) as a potential adsorbent and sensor for the removal and detection of picric acid contaminant: DFT Studies. Cent Asian J Environ Sci Technol Innov. 2021, 2. DOI: 10.22034/CAJESTI.2021.01.02.
40. Awan B, Sabeen M, Shaheen S, Mahmood Q, Ebadi A, Toughani M. Phytoextraction of zinc contaminated water by Tagetes minuta L. Cent Asian J Environ Sci Technol Innov. 2020;1:150–158. DOI: 10.22034/CAJESTI.2020.03.04.
41. Bafkar A. Kinetic and equilibrium studies of adsorptive removal of sodium-ion onto wheat straw and rice husk wastes. Cent Asian J Environ Sci Technol Innov. 2020, 1. DOI: 10.22034/CAJESTI.2020.06.04.
42. Maina Y, Kyari B, Jimme M. Impact of household fuel expenditure on the environment: The quest for sustainable energy in Nigeria. Cent Asian J Environ Sci Technol Innov. 2020;1:109–118. DOI: 10.22034/CAJESTI.2020.02.06.
43. Nwankwo C, EGobo A, Israel-Cookey C, AAbere S. Effects of hazardous waste discharge from the activities of oil and gas companies in Nigeria. Cent Asian J Environ Sci Technol Innov. 2020;1:119-129. DOI: 10.22034/CAJESTI.2020.02.07.
44. Qayyum S, Khan I, Meng K, Zhao Y, Peng C. A review on remediation technologies for heavy metals contaminated soil. Cent Asian J Environ Sci Technol Innov. 2020;1:21-29. DOI: 10.22034/CAJESTI.2020.01.03.
45. Ebadi A, Toughani M, Najafi A, Babaee M. A brief overview on current environmental issues in Iran. Cent Asian J Environ Sci Technol Innov. 2020;1:1–11. DOI: 10.22034/CAJESTI.2020.01.08.
46. Nnaemeka A. Environmental pollution and associated health hazards to host communities (Case study: Niger delta region of Nigeria). Cent Asian J Environ Sci Technol Innov. 2020;1:30–42. DOI: 10.22034/CAJESTI.2020.01.04.
47. Firozjaii AM, Saghafi HR. Review on chemical enhanced oil recovery using polymer flooding: Fundamentals, experimental and numerical simulation. Petroleum; c2020. DOI: 10.1016/j.petlm.2019.09.003.
48. Mandal A. Chemical flood enhanced oil recovery: A review. Int. J Oil Gas Coal Technol; c2015. DOI: 10.1504/IJOGCT.2015.069001.
49. Gurgel A, Moura MCPA, Dantas TNC, Neto EB, Neto AD. A review on chemical flooding methods applied in enhanced oil recovery. Braz J Pet Gas; c2008. DOI: 10.5419/bjpg.v2i2.53.
50. Davarpanah A, Mirshekari B. Mathematical modeling of injectivity damage with oil droplets in the waste produced water re-injection of the linear flow. Eur Phys J Plus; c2019. DOI: 10.1140/epjp/i2019-12546-9.
51. Davarpanah A, Shirmohammadi R, Mirshekari B, Aslani A. Analysis of hydraulic fracturing techniques: Hybrid fuzzy approaches. Arabian J Geosci. 2019. DOI: 10.1007/s12517-019-4567-x.
52. Esfandyari H, Moghani Rahimi A, Esmaeilzadeh F, Davarpanah A, Mohammadi AH. Amphoteric and

cationic surfactants for enhancing oil recovery from carbonate oil reservoirs. J Mol Liq; c2020. DOI: 10.1016/j.molliq.2020.114518.
53. Davarpanah A, Mirshekari B. Numerical simulation and laboratory evaluation of alkali–surfactant–polymer and foam flooding. Int J Environ Sci Technol; c2019. DOI: 10.1007/s13762-019-02438-9.
54. Davarpanah A, Mirshekari B. Experimental study of CO2 solubility on the oil recovery enhancement of heavy oil reservoirs. J Therm Anal Calorim; c2019. DOI: 10.1007/s10973-019-08498-w.
55. Esfandyari H, Shadizadeh SR, Esmaeilzadeh F, Davarpanah A. Implications of anionic and natural surfactants to measure wettability alteration in EOR processes. Fuel; c2020. DOI: 10.1016/j.fuel.2020.118392.
56. Davarpanah A, Mirshekari B. A mathematical model to evaluate the polymer flooding performances. Energy Rep; c2019. DOI: 10.1016/j.egyr.2019.09.061.
57. Esfandyari H, Hoseini AH, Shadizadeh SR, Davarpanah A. Simultaneous evaluation of capillary pressure and wettability alteration based on the USBM and imbibition tests on carbonate minerals. J Pet Sci Eng. 2020. DOI: 10.1016/j.petrol.2020.108285.
58. Hu Y, Cheng Q, Yang J, Zhang L, Davarpanah A. A laboratory approach on the hybrid-enhanced oil recovery techniques with different saline brines in sandstone reservoirs. Processes. 2020;8:1051. DOI: 10.3390/pr8091051.
59. Davarpanah A, Shirmohammadi R, Mirshekari B. Experimental evaluation of polymer-enhanced foam transportation on the foam stabilization in the porous media. Int. J Environ Sci. Technol; c2019. DOI: 10.1007/s13762-019-02280-z.
60. Davarpanah A, Akbari E, Doudman-Kushki M, Ketabi H, Hemmati M. Simultaneous feasible injectivity of foam and hydrolyzed polyacrylamide to optimize the oil recovery enhancement. Energy Explor Exploit; c2019. DOI: 10.1177/0144598718786022.
61. Haiyan Z., Davarpanah A. Hybrid Chemical Enhanced Oil Recovery Techniques: A Simulation Study. Symmetry. 2020;12:1086. DOI: 10.3390/sym12071086.
62. Sheng JJ. Modern Chemical Enhanced Oil Recovery. Mod. Chem. Enhanc. Oil Recover; c2011. DOI: 10.1016/C2009-0-20241-8.
63. Hu Z, Haruna M, Gao H, Nourafkan E, Wen D. Rheological properties of partially hydrolyzed polyacrylamide seeded by nanoparticles. Ind Eng Chem Res. 2017;56(24):7056-7065. DOI:10.1021/acs.iecr.6b05036.
64. Agista MN, Guo K, Yu Z. A state-of-the-art review of nanoparticles application in petroleum with a focus on enhanced oil recovery. Appl Sci. 2018;8(6):871. DOI:10.3390/app8060871.
65. Shamsijazeyi H, Miller CA, Wong MS, Tour JM, Verduzco R. Polymer-coated nanoparticles for enhanced oil recovery. J Appl Polym Sci. 2014;131(19):40576. DOI:10.1002/app.40576.
66. Ali JA, Kolo K, Manshad AK, Mohammadi AH. Recent advances in application of nanotechnology in chemical enhanced oil recovery: effects of nanoparticles on wettability alteration, interfacial tension reduction, and flooding. Egypt J Pet. 2018;27(3):569-577. DOI:10.1016/j.ejpe.2018.09.006.
67. Cheraghian G, Hendraningrat L. A review on applications of nanotechnology in the enhanced oil recovery part B: Effects of nanoparticles on flooding. Int Nano Lett. 2016;6(1):1-10. DOI:10.1007/s40089-015-0170-7.
68. Ali JA, Kalhury AM, Sabir AN, Ahmed RN, Ali NH, Abdullah AD. A state-of-the-art review of the application of nanotechnology in the oil and gas industry with a focus on drilling engineering. J Pet Sci Eng. 2020;189:107118. DOI:10.1016/j.petrol.2020.107118.
69. Ju B, Fan T, Ma M. Enhanced oil recovery by flooding with hydrophilic nanoparticles. China Particuology. 2006;4(2):118-122. DOI:10.1016/S1672-2515(07)60232-2.
70. Ogolo NA, Olafuyi OA, Onyekonwu MO. Enhanced oil recovery using nanoparticles. SPE Saudi Arab Sect Tech Symp Exhib. 2012; DOI:10.2118/160847-ms.
71. Piñerez Torrijos ID, Puntervold T, Strand S, Austad T, Bleivik TH, Abdullah HI. An experimental study of the low salinity Smart Water-Polymer hybrid EOR effect in sandstone material. J Pet Sci Eng. 2018;163:152-160. DOI:10.1016/j.petrol.2018.01.031.
72. Omidi A, Manshad AK, Moradi S, Ali JA, Sajadi SM, Keshavarz A. Smart- and nano-hybrid chemical EOR flooding using Fe3O4/eggshell nanocomposites. J Mol Liq. 2020;302:113880. DOI:10.1016/j.molliq.2020.113880.
73. Shabib-Asl A, Abdalla Ayoub M, Abdalla Elraies K. Combined low salinity water injection and foam flooding in sandstone reservoir rock: A new hybrid EOR. In: Proceedings of the SPE Middle East Oil and Gas Show and Conference. Manama, Bahrain. 18–21 March 2019.
74. Rezvani H, Panahpoori D, Riazi M, Parsaei R, Tabaei M, Cortés FB. A novel foam formulation by Al2O3/SiO2 nanoparticles for EOR applications: A mechanistic study. J Mol Liq. 2020;302:112730. DOI:10.1016/j.molliq.2020.112730.
75. Maghzi A, Mohebbi A, Kharrat R, Ghazanfari MH. An experimental investigation of silica nanoparticles effect on the rheological behavior of polyacrylamide solution to enhance heavy oil recovery. Pet Sci Technol. 2013;31(12):1301-1314. DOI:10.1080/10916466.2010.518191.
76. Gbadamosi AO, Junin R, Manan MA, Agi A, Oseh JO, Usman J. Effect of aluminium oxide nanoparticles on oilfield polyacrylamide: Rheology, interfacial tension, wettability, and oil displacement studies. J Mol Liq. 2019;274:111863. DOI:10.1016/j.molliq.2019.111863.
77. Ahmed A, Saaid IM, Ahmed AA, Pilus RM, Baig MK. Evaluating the potential of surface-modified silica nanoparticles using internal olefin sulfonate for enhanced oil recovery. Pet Sci. 2020;17(4):799-811. doi:10.1007/s12182-019-00404-1.
78. Sun X, Zhang Y, Chen G, Gai Z. Application of nanoparticles in enhanced oil recovery: A critical review of recent progress. Energies. 2017;10(3):345. DOI:10.3390/en10030345.
79. Gbadamosi AO, Junin R, Manan MA, Yekeen N, Agi A, Oseh JO. Recent advances and prospects in polymeric nanofluids application for enhanced oil recovery. J Ind Eng Chem. 2018;66:51-70. DOI:10.1016/j.jiec.2018.05.020.
80. Ali H, Soleimani H, Yahya N, Khodapanah L, Sabet M, Demiral BMR, *et al*. Enhanced oil recovery by using electromagnetic-assisted nanofluids: A review. J Mol Liq. 2020;303:113095. DOI:10.1016/j.molliq.2020.113095.
81. Gbadamosi AO, Junin R, Manan MA, Agi A, Oseh JO, Usman J. Synergistic application of aluminium oxide nanoparticles and oilfield polyacrylamide for enhanced oil recovery. J Pet Sci Eng. 2019;177:106345. DOI:10.1016/j.petrol.2019.106345.
82. Maurya NK, Mandal A. Studies on behavior of suspension of silica nanoparticle in aqueous

polyacrylamide solution for application in enhanced oil recovery. Pet Sci Technol. 2016;34(10):868-876. DOI:10.1080/10916466.2016.1145693.
83. Cheraghian G, Khalili Nezhad SS, Kamari M, Hemmati M, Masihi M, Bazgir S. Adsorption polymer on reservoir rock and role of the nanoparticles, clay and SiO2. Int Nano Lett. 2014;4(1):1-11. DOI:10.1007/s40089-014-0114-7.
84. Saha R, Uppaluri RVS, Tiwari P. Impact of Natural Surfactant (Reetha), Polymer (Xanthan Gum), and Silica Nanoparticles to Enhance Heavy Crude Oil Recovery. Energy Fuels. 2019;33(9):8692-8702. DOI:10.1021/acs.energyfuels.9b00790.
85. Sharma T, Iglauer S, Sangwai JS. Silica nanofluids in an oilfield polymer polyacrylamide: Interfacial properties, wettability alteration, and applications for chemical enhanced oil recovery. Ind Eng Chem Res. 2016;55(42):11259-11268. DOI:10.1021/acs.iecr.6b03299.
86. Lee J, Huang J, Babadagli T. Visual support for heavy-oil emulsification and its stability for cold-production using chemical and nanoparticles. In: Proceedings of the SPE Annual Technical Conference and Exhibition. Calgary, AB, Canada. 30 September–2 October 2019.
87. Cheraghian G. Evaluation of clay and fumed silica nanoparticles on adsorption of surfactant polymer during enhanced oil recovery. J Jpn Pet Inst. 2017;60(2):85-92. DOI:10.1627/jpi.60.85.
88. Samba MA, Hassan HA, Munayr MS, Yusef M, Eschweido A, Burkan H, *et al*. Nanoparticles EOR aluminum oxide (Al2O3) used as a spontaneous imbibition test for sandstone core. In: Proceedings of the ASME International Mechanical Engineering Congress and Exposition. Salt Lake City, UT, USA. 11–14 November 2019.
89. Daryayehsalameh B, Nabavi M, Vaferi B. Modeling of CO2 capture ability of [Bmim][BF4] ionic liquid using connectionist smart paradigms. Environ Technol Innov. 2021;22:101484. DOI:10.1016/j.eti.2021.101484.